Identification of Adeno-Associated Virus Variants for Gene Transfer Into Human Neural Cell Types by Parallel Capsid Screening

Lea Jessica Flitsch
University of Bonn Medical Faculty & University Hospital Bonn
Kathleen Börner
Heidelberg University
Christian Stüllein
CLADIAC GmbH
Simon Ziegler
CLADIAC GmbH
Vera Sonntag-Buck
Heidelberg University
Vesselina Semkova
University of Bonn Medical Faculty & University Hospital Bonn
Si Wah Christina Au Yeung
University of Bonn Medical Faculty & University Hospital Bonn
Julia Schlee
University of Bonn Medical Faculty & University Hospital Bonn
Mohamad Hajo
University of Bonn Medical Faculty & University Hospital Bonn
Mona Mathews
LIFE & BRAIN GmbH
Dirk Grimm
Heidelberg University
Oliver Brüstle (✉ brustle@uni-bonn.de)
University of Bonn Medical Faculty & University Hospital Bonn

Research Article

Keywords: NGN2, vitrocell, neuralprogenitors, SLC25A1, (iNSCs)

Posted Date: September 2nd, 2021

DOI: https://doi.org/10.21203/rs.3.rs-861785/v1

Abstract

Human brain cells generated by *in vitro*cell programming provide exciting prospects for disease modeling, drug discovery and cell therapy. These applications frequently require efficient and clinically compliant tools for genetic modification of the cells. Recombinant Adeno-associated viruses (AAVs) fulfill these prerequisites for a number of reasons, including the availability of a myriad of AAV capsid variants with distinct cell type specificity (also called tropism). Here, weharnessed a customizable parallel screening approach to assessa panel of natural or synthetic AAV capsid variants for their efficacy in lineage-related human neural cell types.We identified common lead candidates suited for the transduction of directly converted,early-stage induced neural stem cells (iNSCs), induced pluripotent stem cell (iPSC)-derived later-stage, radial glia-like neuralprogenitors,as well as differentiated astrocytic and mixed neuroglial cultures.We then selected a subsetof these candidates for functional validation in iNSCs and iPSC-derived astrocytes, usingshRNA-induced downregulation of the citrate transporter SLC25A1 and overexpression of the transcription factor NGN2 for proofs-of-concept. Our study provides a comparative overview ofthe susceptibility of different human cell programming-derived brain cell types to AAV transduction and a critical discussionof the assets and limitations of the specific AAV capsidscreening approach.

1. Introduction

Ever since the groundbreaking introduction of the induced pluripotent stem cell (iPSC) reprogramming technology by Kazutoshi Takahashi and Shinya Yamanaka[1,2], the field of cell programming has constantly evolved and given rise to a plethora of different techniques, which can now be used to derive, for instance, brain cells for biomedical applications. These techniques comprise strategies using morphogens and/or transcription factors to differentiate iPSCs into the desired cell types[3], as well as direct conversion approaches enabling transdifferentiation of one somatic cell type into another without a pluripotent intermediate.[4] Next to their use as human cellular platforms for disease modelling[5], cell programming-derived human cells are promising donor sources for cell replacement strategies[6]. Clinical benefit may also be achieved directly *in vivo*, for instance, through the conversion of brain-resident glial cells into neurons.[7,8] In that regard, the implementation of efficient and safe-in-human transgene delivery methods represents a crucial prerequisite for further advancing cell programming approaches towards clinical application.

Recombinant Adeno-associated viruses (AAVs) are well suited transgene delivery systems for cell programming and engineering, owing to a number of unique assets, including their high versatility.[9,10] The latter is based on the availability of a wealth of natural or synthetic AAV capsids, which, combined with the ease of AAV DNA and protein engineering, offers a great assortment of AAV variants suitable for biomedical applications.[11,12] Notably, swapping the AAV capsid ('pseudotyping') can affect both, transduction efficiency and cell type specificity[13,14], and the outcomes can also differ between species[15]. This provides the option to screen capsid pools *in vitro* or *in vivo*, and to identify the best AAV variant for

a given species and organ or cell type of interest. For example, in a previous study, human embryonic stem cells (ESCs) and iPSCs, as well as ESC- and iPSC-derived cardiomyocytes were transduced with AAVs of four different serotypes (AAV1, AAV2, AAV6 and AAV9) at three different MOIs (multiplicity of infections). Despite the observation of a significant degree of cell death in undifferentiated cells and much higher absolute transduction efficiencies in differentiated cells, serotypes AAV2 and AAV6 performed best across groups. In a direct comparison of transduction efficiencies of these two AAV variants to lentiviral and adenoviral vectors expressing enhanced green fluorescent protein (EGFP), the adenoviral vectors were superior in undifferentiated cells, whereas ESC- and iPSC-derived cardiomyocytes were best transduced with the tested AAVs.[16] More recently, transduction efficiencies of 11 different AAV capsid variants (AAV1 through AAV9, AAV7m8 and AAV8b) were assessed in human iPSCs, iPSC-derived retinal pigment epithelium and human iPSC-derived as well as rat primary cortical neurons. Measurement of AAV-mediated EGFP expression after transduction at three MOIs and four different time points showed that AAV7m8 performed best across all cell types and MOIs analyzed. Notably, substantial differences in absolute expression levels and time of expression onset were observed between species and cell types.[15]

These and other studies demonstrate that AAV tropism and means for the identification of ideal capsids, as well as transgenes and delivery routes, are pivotal for the success of AAV applications in neural cell types.[17] Curiously, despite significant advances in technologies for directed molecular AAV capsid evolution over the last two decades[11,18], systematic comparative studies of the increasing numbers of available AAV variants remain scarce. To tackle this shortcoming, some of us have recently established pre-arrayed pan-AAV peptide display libraries in 96-well format and demonstrated the capacity of this platform to rapidly and efficiently screen AAV variants in over 90 transformed or primary cell types of different species.[19] Here, we employed this customizable parallel approach to screen for AAV variants yielding high transduction efficiencies in lineage-related human neural cell types. We specifically included directly converted and iPSC-derived neural stem cells (NSCs) of distinct developmental stages, neurons and/or astrocytes derived thereof, and forward programmed neurons. For most cell types, we could identify AAV capsid variants mediating better transduction efficiency than their respective wild-type parental capsid. Furthermore, we verified that the identified lead candidates were suitable for loss- or gain-of-function studies, such as gene knockdown or transgene overexpression, respectively.

2. Results

Identification of lead AAV capsids for transduction of human neural cell types through parallel screening

In this study, we harnessed a recently established, customizable parallel screening platform in 96-well format to identify AAV capsid variants that mediate robust transduction efficiency in neural cell types. We focused on screening cell programming-derived human neural cell types, which are good proxies for hardly accessible primary human brain cells, and which, thus, are at the center of recent biomedical efforts in the area of disease modelling, drug screening and neuroregeneration. To represent the variety of available cell programming techniques that have been established over the last decades as well as the

diversity of human neural cell types and stages, we included the following lineage-related populations in our study (Fig. 1a): (i) Two types of non-polarized, early-stage NSCs derived via either direct cell fate conversion or small molecule-driven differentiation of iPSCs. In the first case, we used induced neural stem cells (iNSCs), which are tripotent *bona fide* NSCs derived from human adult blood cells by direct conversion utilizing overexpression of the two transcription factors SOX2 and cMYC.[20] In the second case, we employed small molecule-derived neural precursor cells (smNPCs), which are self-renewing NSCs generated from iPSCs by using small molecules impacting BMP, TGFβ, GSK3 and SHH signaling.[21] (ii) A polarized EGF- and FGF-dependent neural precursor population, which is derived from iPSCs by manual selection and propagation of neural rosettes.[22] Moreover, differentiated neuroglial cultures generated from these so-called long-term neuroepithelial-like stem cells (ltNES) were assessed. (iii) Late-stage, radial glia-like neural precursor cells (RGL-NPCs), which are generated from iPSCs via retinoic acid-treated embryoid bodies, and which can be differentiated into almost pure astrocytic cultures due to their strong gliogenic potential.[23] (iv) Neuronal cultures derived from iPSCs via transcription factor-mediated forward programming. Specifically, we either overexpressed the neurogenic transcription factor NGN2 alone or a combination of ASCL1 plus DLX2.[24] In addition to these neuroectodermal cell types, we performed AAV screening in iPSC-derived microglia (iPSdMiG), since these mesodermal lineage cells are the immune cells of the central nervous system (CNS), and as such relevant for a number of neurological, neuropsychiatric and neurodegenerative diseases.

All cell types were subjected to AAV screening using a library of AAV capsid variants encoding a yellow fluorescent reporter (YFP) driven by a strong cytomegalovirus (CMV) promoter, and pre-arrayed in a 96-well plate cell culture format. As recently reported by some of us[19], this technology platform enables the side-by-side comparison of synthetic AAV capsid variants of interest to their respective wild-type AAVs as well as to published AAV benchmarks, using flow cytometry- or microscopy-based measurement of YFP fluorescence as readout for transduction rate (percentage of YFP-positive cells) and expression strength (YFP intensity per cell). Here, we used a particular subset of our reported libraries that comprised 12 AAV wild-types (AAV1 through AAV9, AAVpo1, AAVrh10 and AAV12) as well as an assortment of pan-AAV peptide display variants, *i.e.*, capsids whose tropism has been altered by insertion and display of short, seven or nine amino acids long peptides in an exposed region on the capsid surface (overviews on all introduced modifications and insertion sites are provided in Supplementary Tables 1 and 2, respectively). These selected AAV variants were among the best performers in our recently reported screen on a variety of cell types, including primary murine CNS cells and human astrocytes[19], and hence deemed suitable and promising for the present work. For screening, cells were plated in 96-well plates and transduced with equal amounts of all AAV capsid variants. Forty-eight hours later, the plates were fixed and subjected to fluorescence measurements using a plate reader and/or microscopy including automated image acquisition and analysis, in order to determine the transduction efficiency and absolute YFP expression of each screened AAV variant. Notably, while both screening readouts demonstrated a strong positive correlation ($p < 2.2e\text{-}16$, $\tau = 0.777$), the latter technique yielded data with greater resolution (Supplementary Fig. S1).

This workflow enabled us to identify several capsid variants that performed well in iNSCs (Fig. 1b, c), ltNES-derived neuroglial differentiation cultures (Fig. 1d), as well as RGL-NPCs (Fig. 1e) and RGL-NPC-derived astrocytes (Fig. 1f). Two genetically distinct smNPC lines and undifferentiated ltNES were also transduced by a subset of AAV variants albeit the YFP expression levels were lower than in the aforementioned cell types. The only cell types that were inefficiently transduced by any of the screened AAV variants were forward programmed NGN2- and ASCL1/DLX2-neurons, as well as iPSdMiG (Supplementary Fig. S2).

Intrigued by this finding, we next set out to investigate whether neurons were transduced within ltNES-derived mixed neuroglial cultures, or whether this cell type might be generally resistant to AAV transduction. To this end, we first stained our screening plate against the pan-neuronal marker TUBB3 48 hours after transduction, and were indeed able to identify TUBB3/YFP-double-positive cells (Supplementary Fig. S3). The 96-well screening could not be used to characterize YFP-expressing cells in ltNES-derived mixed neuroglial cultures in greater depth using a more comprehensive marker panel though, because the AAV-YFP screening already occupied three fluorescence channels, which is why only one marker could additionally be stained at a time per screening plate. Therefore, these cells were next seeded in 3.5 cm staining dishes and transduced with a pool of three GFP-encoding AAVs (AAV1P2, 7P2 and 8P2). These AAV variants were identified as lead candidates for the transduction of differentiated ltNES in our previously performed screen. Accordingly, in analogy to the conducted screening, cells were fixed 48 hours after transduction and stained for markers of NSCs, glial cells and differentially mature neurons. Quantification of immunofluorescent stainings revealed that AAVs transduced especially NSCs and immature TUBB3-positive neurons in this mixed neuroglial culture, whilst transduction efficiencies decreased in more mature MAP2-positive neurons and astrocytes (Supplementary Fig. S3).

In all robustly transduced cell types (Fig. 1c - f), we found peptide-modified AAV capsid variants that surpassed their respective wild-type capsid in terms of transduction efficiency, including serotypes AAV1, AAV2 or AAV6 that frequently perform well in a wide range of different cell types[19]. More specifically, our best hits comprised serotypes AAV1 and AAV6, whose capsid proteins only vary from each other in a few amino acids[25], modified with peptides P2, P4 and P5, as well as serotypes AAV7, AAV8, AAV9 and AAVrh10 modified with peptides P2, A2 and A6. Amongst the shared hits, AAV7P2 was the most promising lead candidate as it efficiently transduced iNSCs, ltNES-derived differentiation cultures, RGL-NPCs and RGL-NPC-derived astrocytes (Fig. 1g).

Remarkably, especially the P2 peptide modification greatly increased the transduction efficiency of all screened serotypes except for AAV4, AAV5, AAVpo1 and AAV12. Since the P2 peptide sequence CDC**RGD**CFC includes an RGD motif known to be involved in integrin binding [26–28], we followed up on this observation using our previously published RNA sequencing data set[20] to profile expression levels of integrin protein family members in iNSCs, smNPCs and blood cells. As iNSCs were robustly transduced by P1 (**RGD**LGLS)- and P2 (CDC**RGD**CFC)-displaying AAV variants, we further used qPCR to assess the expression levels of *ITGA6*, *ITGAE, ITGB1*, *ITGB5* and *ITGB8*, which were the most strongly expressed integrins in iNSCs (Supplementary Fig. S4). We were specifically interested in comparing expression

levels of well-transducible (iNSCs, ltNES-derived differentiation cultures, RGL-NPCs, astrocytes) and difficult-to-transduce (smNPCs, ASCL1/DLX2-neurons, iPSdMiG) cell types. Indeed, we observed a trend toward higher *ITGB8* expression in well-transducible cell types, whereas no evidence for a correlation was detected for the other integrins investigated.

Validation of the ability of selected AAV capsid variants to modulate gene expression in human neural cells

We next aimed to verify the potential of selected lead candidates identified in our screen by employing them for loss- or gain-of-function studies. To this end, we first chose the four lead AAV variants AAV1P2, 7P2, 8P2 and 9P1 to explore their efficiency in a knockdown scenario in human iNSCs. As an example, we targeted SLC25A1, which is a mitochondrial carrier exchanging citrate for malatate and as such relevant for the production of acetyl CoA, one of the key players in cell metabolism[29,30]. We employed equal amounts of crude lysates (*i.e.*, non-purified extracts from cells transfected with all plasmids required for AAV production) of these four AAV variants expressing GFP and shRNA targeting SLC25A1 (shSLC) or a non-silencing control (Ctrl). Forty-eight hours after transduction, flow cytometry revealed that all tested variants transduced iNSCs with very high efficiencies ranging from 97.4–98.4% (Fig. 2a). Furthermore, in shSLC-transduced cultures, *SLC25A1* expression was nearly abolished on the RNA level as compared to controls (Fig. 2b).

In a second example, we used purified and concentrated AAV7P2 vectors to overexpress the neurogenic transcription factor NGN2 in iNSCs and astrocytes. We expected NGN2 overexpression to promote neuronal fate acquisition, since it was shown that overexpression of this transcription factor alone suffices to induce rapid neuronal fate acquisition of iPSCs *in vitro*[31] and even converts glia into neurons *in vivo*[32]. In both cell types investigated, *NGN2* expression levels were highly elevated, *i.e.*, roughly 8,500-fold after transduction of iNSCs (Fig. 2c) and around 252,000-fold after transduction of astrocytes (Fig. 2d), as compared to the respective untransduced controls. As expected, AAV7P2-mediated overexpression of NGN2 biased spontaneous differentiation of iNSCs towards a neuronal fate over a period of two weeks. This was evident, for example, from the almost seven-fold elevated expression of *PAX6*, a master regulator of later stage NSC proliferation and neurogenesis, and a known inducer of NGN2[33–40]. Furthermore, expression levels of the neuronal markers *TUBB3*, *MAP2* and *NEUN* were increased, whilst the astrocyte marker *GFAP* was downregulated upon NGN2 overexpression (Fig. 2c). This was further supported by immunofluorescence studies, which showed that NGN2-overexpressing iNSC cultures displayed more prominent expression of the neuronal markers TUBB3 and MAP2 (Fig. 2e). Along the same line, NGN2 overexpression in iPSC-derived astrocytes resulted in a three- to seven-fold increase in the expression levels of the neuronal markers *TUBB3*, *NEUN* and *MAP2* on bulk RNA level (Fig. 2d). This sufficed to initiate cell fate conversion in a fraction of the cultured astrocytes, as single MAP2-positive cells with neuronal morphology were detectable two weeks after AAV7P2 transduction (Fig. 2f).

Collectively, these proof-of-principle experiments demonstrate the power of our parallel screening approach in 96-well format to identify synthetic AAV capsid variants that can be employed to modulate gene expression in different human programmed CNS cell types.

3. Discussion

Here, we have capitalized on our recent establishment of a pre-arrayed parallel AAV screening pipeline[19] and used this to identify AAV capsid variants with high transduction efficiency in diverse human cell programming-derived CNS cell types. Our two major findings are that most of the cell types screened are highly amenable to AAV transduction, and that our parallel screening format can identify lead candidates, which convey better transduction than their parental wild-type serotypes.

Notably though, some cell types, including forward programmed NGN2- as well as ASCL1/DLX2-neurons, were not efficiently transduced by our specific AAV panel. Possible explanations are that these cell types are generally resistant to AAV transduction or require a higher AAV dose than what is provided by the non-concentrated crude lysates in our pre-arrayed screening plates. In this context, it is interesting to note that, although purified cultures of forward programmed neurons were not efficiently transduced by our AAV screening panel, immunofluorescence analysis of AAV-transduced ltNES-derived neuroglial cultures revealed that especially NSCs and less mature human neurons are, in principle, amenable to AAV transduction. Our results are overall in line with previous data showing that in both, iPSC-derived as well as primary human cell cultures, AAV9P1 (a peptide display variant of AAV9 that was also included in the present panel) yields lower transduction rates in neurons as compared to astrocytes.[14] Moreover, it has been reported that transduction efficiencies of 11 different AAV variants are much lower for human iPSC-derived than rat primary cortical cultures[15], which also supports the notion that human neurons are difficult to transduce with AAVs. Interestingly, in this published screen, AAV-mediated EGFP expression in human iPSC-derived neurons was first detected at 96 hours after transduction with the highest MOI tested (10^6 viral genomes (vg)/cell).[15] Thus, the poor neuronal transduction rates observed in our forward programmed neuron screens could be due to low virus concentrations in the crude lysates, a too short follow-up (48 hours post-transduction) in this screen and/or a too advanced neuronal maturation state acquired by forward programmed neurons at the time of AAV transduction. These findings are concordant with others, altogether indicating that transduction patterns in mature neurons are species-specific and could, at least *in vivo*, potentially even depend on the age of an organism at the time of AAV treatment.[17]

In addition to these limitations, it is key to realize that the pivotal benefits of our screening platform, *i.e.*, its speed and ease, come at the prize of a limited capsid diversity in the original panel. Unlike a conventional directed evolution approach that typically starts with a complex library of millions of distinct AAV variants, which is then iteratively screened on target cells over multiple rounds of infection and rescue, our current approach is based on a much smaller library of pre-selected capsid variants encoding a reporter, thus enabling a rapid read-out after a single screening round. Hence, it is well

possible that the cell lines that came back negative in our current screens are still transducible by other AAV capsid variants that were lacking in our present panel. Nevertheless, systematic screening approaches in lineage-related cell types, such as the one employed in this study, could be valuable as a basis to select the most promising AAV variants for subsequent studies aiming at further enhancing AAV performance in a model-orientated manner. For example, directed evolution was previously used to generate an AAV2/AAV5 chimera with an A581T point mutation, which is highly specific to and infectious in an organotypic human airway model[41]. Similar studies have already been conducted *in vitro* for human pluripotent stem cells[42] and rat primary as well as human ESC-derived neural precursor cells[43], and even *in vivo* targeting different mouse brain cell types[44].

Considering the inherent trade-off of the pros and cons of this particular parallel AAV screening strategy, it is noteworthy that the ability to compare a custom-built selection of AAV variants across various cell types could also be valuable for identifying, for instance, AAV cell entry mechanisms that might be common for several capsid variants in lineage-related cell types. In this regard, recurrent patterns in capsid modifications yielding increased transduction efficiencies could be particularly relevant. In line with this, our preliminary data could suggest that integrin binding might represent an interesting mechanism to investigate further in future studies.

Lastly, we demonstrate that top hits identified by parallel AAV screening not only excel at the transduction of a reporter gene, but can also be harnessed to functionally modulate gene expression in neural cells. For example, we identified and verified the AAV peptide display variants AAV1P2, 7P2, 8P2 and 9P1 as lead candidates for the transduction of human iNSCs. These results are in line with one of our previous studies where 30 AAV variants – which are also included in the current screening panels – were used for the transduction of HNSC.100 cells kept as proliferating NSCs or differentiated astrocyte-enriched cultures, and which identified AAV9P1 as the variant yielding the highest transduction efficiencies.[14] Importantly though, one remaining key question is whether and to what extent screening results obtained in simplified 2D *in vitro* systems can predict *in vivo* functionality and thus clinical translatability. Here, it is worth noting that the wild-type form of AAV9 – which was the first AAV serotype described to be capable of bypassing the blood-brain-barrier[17] – or a capsid-modified variant thereof (*i.e.*, AAV9P1) have already been used *in vitro* in more complex, iPSC-derived 3D organoid models[14,45], as well as *in vivo* to treat mice suffering from either ischemic brain injury[46] or Huntington's disease[47] by mediating astrocyte-to-neuron cell fate conversion. On top of this, two of our recently published studies illustrate that the screening approach employed here is even applicable *in vivo* when combined with molecular barcoding and next-generation sequencing.[48,49] For instance, injecting 177 barcoded AAV-YFP variants (representing a library that is significantly overlapping with the one used in this study) into the lateral ventricle of adult mice enabled the identification of two lead candidates, namely AAV variants 9A2 and 1P5, capable of efficiently transducing NSCs in the ventral subventricular zone.[49]

It is finally interesting to note that AAV9A2 and 1P5, which we identified as lead candidates in our recent study in endogenous mouse NSCs[49], were outperformed by other capsid variants in human iNSCs and

iPSC-derived RGL-NPCs in the present work. This notion again stresses the cell type- and species-specificity of AAV transduction and the ensuing need to always evaluate the performance of available AAV variants within the proper context, for instance by means of parallel capsid screening as exemplified here. Since it was recently shown that capsid-promoter interactions can significantly impact AAV tropism *in vivo*[50], it can be foreseen that the customizable combination of capsid-modified AAV lead candidates with selective promoters and/or miRNAs could be used to boost the cell type-specificity that can be achieved by AAV variants. This might fuel further attempts to target one out of multiple cell types present in more complex CNS models such as cerebral organoids or even in native brain tissue.

4. Methods

Cell culture

All human cell programming-derived neural cell types were generated, cultured and/or expanded using previously described methods: iNSCs[20], smNPCs[21], ltNES[22], RGL-NPCs[23], as well as forward programmed NGN2- and ASCL1/DLX2-neurons[24]. IPSdMiG were generated via a proprietary protocol from LIFE & BRAIN GmbH (patent application number EP20162230). Details are found in the Supplementary Methods.

AAV production and transduction

AAV vectors were produced in HEK293T cells using a standard triple-transfection protocol and an AAV helper plasmid encoding AAV *rep* and *cap* genes, an AAV vector plasmid carrying the transgene as well as an adenoviral helper plasmid.[51] Wild-type *cap* genes were modified through insertion of DNA oligonucleotides encoding 7mer or 9mer peptides whose sequences and properties were reported[19] and are provided in Supplementary Table S1.

For parallel AAV capsid screening in 96-well plate format, crude cell lysates from triple-transfected 6-well plates containing non-purified AAV particles were used. Therefore, 10 µl AAV were added per well with a multichannel pipette directly into the medium (200 µl) of the pre-plated cells (1:20 dilution). For the characterization of ltNES-derived neuroglial differentiation cultures and AAV-mediated gene knockdown, cells were cultured in 3.5 cm dishes and transduced with crude lysates at a 1:20 dilution.

For purification by iodixanol gradient density centrifugation, cells were collected by scraping 72 hours after transfection, followed by centrifugation at 500 × g for 15 minutes at room temperature. The cell pellet was resuspended in 20 ml Benzonase buffer and lysed by five freeze-thaw cycles in liquid nitrogen and a 37°C water bath. Cell debris was sonicated for 1 minute and subjected to two centrifugations steps, each at 4,000 × g for 15 minutes at 4°C. The virus-containing lysate was purified via iodixanol density gradient ultracentrifugation (290,000 × g, 120 minutes, 4°C) and collection of the 40% phase. This AAV-containing fraction was rebuffered in 1xDPBS using amicon spin columns (Merck, Darmstadt, Germany) and AAVs were stored in aliquots at -80°C. Viral genome titers were determined by qPCR using the AAV

quantification kit from Norgen Biotek Corporation (Ontario, Canada). Concentrated AAVs were used for NGN2 overexpression at a dose of $6x10^4$ vg/cell.

Cloning procedures

To generate an AAV vector expressing an shRNA against SLC25A1, two complementary oligonucleotides were designed, each comprising the sense (5'-GCCATCCGCTTCTTCGTCATGA-3') and antisense strand (5'-TCATGACGAAGAAGCGGATGGC-3'), as well as the central loop sequence TCAAGAG. The 5’ ends were flanked by the sequence CACC on the forward strand and by AAAA on the reverse strand. Following annealing, these flanking sequences produced overhangs that were used for direct ligation using a Golden Gate protocol into the BbsI-digested AAV vector plasmid TRISPR[52] (details of this plasmid will be reported elsewhere).

To clone the pAAV-EF1a-NGN2-3xFLAG expression vector, plasmids pAAV-EF1a-NGN2-RFP-NLS (details of this plasmid will be reported elsewhere) and NR6AI-C-term-3xFLAG (kindly provided by Nils Braun) were used as templates. The NGN2 and 3xFLAG sequences in these plasmids were PCR-amplified with appropriate overhangs for cloning using primers 5'-tgtcgtgaggaatttcgacggatccgccaccatgttcg-3' plus 5'-ctttataatctttatcatcatcatctttataatcgatacaatccctggctatgg-3' (for NGN2) or 5'-ccatagccagggattgtatcgattataaagatgatgatgataaagattataaag-3' plus 5'-ttcaacatgcctccgcccttatcatttatcatcatcatctttataatc-3' (for 3xFLAG). Gibson assembly was performed using the 2x Gibson assembly master mix (New England Biolabs, Frankfurt am Main, Germany). Thermo Fisher Scientific’s (Waltham, USA) plasmid DNA Miniprep and Maxiprep kits were used for DNA isolation.

Immunocytochemistry

Forty-eight hours after transduction with the AAV panels, cells were washed once with 1xDPBS before fixation with 4% PFA for 10 minutes at room temperature. Afterwards, cells were washed once with 1xDPBS before incubation with 2 µg/ml DAPI for 5 minutes at room temperature. DAPI was replaced by 200 µl 1xDPBS per well before YFP fluorescence was measured using an Infinite M Plex plate reader (Tecan Group, Männedorf, Switzerland; at 500 nm excitation and 540 nm emission) and/or immunofluorescence image acquisition and analysis (see below). For all other immunofluorescent stainings, blocking with 0.5% Triton-X and 10% FBS was performed after fixation, followed by overnight incubation with primary antibody solution at 4°C (1:1,000 rabbit GFAP from Merck Millipore, Burlington, USA, Cat. AB5804; 1:100 rabbit MAP2 from Abgent, San Diego, USA, Cat. AP2018E; 1:200 rabbit Nestin (NES) from Bio-techne, Minneapolis, USA, Cat. NB300-265; 1:1,000 mouse S100b from Sigma-Aldrich, St. Louis, USA, Cat. S2535; 1:100 mouse SOX2 from R&D systems, Minneapolis, USA Cat. MAB2018; 1:400 chicken TUBB3 from Merck Millipore, Cat. AB9354; 1:1,000 mouse TUBB3 from Eurogentec, Lüttich, Belgium, Cat. MMS-435P; 1:1,000 rabbit TUBB3 from biolegend, San Diego, USA, Cat. 802001; in 0.3% Triton-X and 5% FBS). The next day, three washing steps with 0.3% Triton-X were performed before secondary antibody solution was incubated for 2 hours at room temperature (1:500 donkey-anti-rabbit AF-647, Cat. A31573; 1:500 goat-anti-chicken AF-647, Cat. A21449; 1:1,000 goat-anti-mouse AF-555, Cat.

A21424; 1:500 goat-anti-mouse AF-647, Cat. A21236; 1:1,000 goat-anti-rabbit AF-488, Cat. A11008; 1:1,000 goat-anti-rabbit AF-555, Cat. A21429; 1:500 goat-anti-rabbit AF-647, Cat. A21244; in 0.3% Triton-X and 5% FBS; all Thermo Fisher Scientific). After three additional washing steps, nuclei were counter-stained with DAPI. Wells were sealed with Mowiol plus DABCO (Carl Roth, Karlsruhe, Germany).

Image acquisition and analysis

Automated image acquisition of 96-well plates was performed on an epifluorescence Scan^R screening microscope equipped with the Scan^R acquisition software (Olympus Biosystems, Münster, Germany) or an INCell analyzer 2200 (GE Healthcare Bio-Sciences Corp, Piscataway, USA) with the respective INCell analyzer 2200 software. 10× and 20× objectives were used with appropriate excitation and emission filters to measure 9 and 16 positions per well, respectively. For AAV screening, Scan^R images were subsequently processed with a previously established pipeline for quantitative image analysis.[53] This yielded the mean gray value of all cells in the analyzed images, total cell counts, and percentages of AAV-positive cells (determined via fluorescent reporter). Non-quantitative image processing of automatically acquired INCell images for qualitative display was performed with defined CellProfiler pipelines running the 'ApplyThreshold' (threshold strategy: manual) and 'RescaleIntensity' (rescaling strategy: divide each image by the same value) modules. Alternatively, images were manually captured with an AxioImager plus Apotome (Carl Zeiss, Oberkochen, Germany) and the AxioVision software. Quantification of manually acquired images was performed using a semi-automated, three-step pipeline specifically developed in the context of this project. 1) Cell segmentation: First, single cells and cell clusters were segmented using the DAPI channel. The segmentation was primary based on adaptive thresholding and Gaussian filtering. Objects were distinguished between invalid objects, cells and cell-clusters depending on size and shape. Cell clusters were broken up into cells by creating distance maps and their local maxima, which were used as the starting point of a watershed algorithm. 2) Background separation: Second, after an initial step of intensity normalization based on the maximum intensity, foreground and background were separated in all other (marker) channels. This could either be done by a thresholding based on intensity quantiles or by fitting Gaussian curves to the intensity distribution. Alternative to two Gaussians (foreground and background), we also found good results when using three Gaussians to distinguish between background, low- and high-expressing cells for some markers stained. Based on the locations of the Gaussians the separation threshold(s) were defined. 3) Classification: Third, the cells identified in step 1 were automatically denotated as marker-positive or -negative by comparison of their mean intensity in the marker channels with a manually set threshold or by probability assignment, if using the Gaussian-fitting approach from step 2. Further options applied to optimize the categorization process comprised measures of texture homogeneity, entropy or energy of objects. As a final step, automatic object categorization could be manually revised, if necessary. After quantification, images were post-processed with ImageJ for display. Image processing included adjustments of brightness and contrast, and was equally applied across single channel pictures.

Flow cytometry

In order to quantify the percentage of successfully transduced cells via flow cytometry, iNSCs were detached and singularized by Accutase (Thermo Fisher Scientific) treatment. GFP fluorescence was measured in FL1 on an Accuri C6 Plus flow cytometer (BD Biosciences, San Jose, USA). Events were gated for living single cells and data analyzed with the associated Accuri C6 Plus analysis software.

qPCR

RNA extraction and cDNA synthesis were performed with Qiagen's (Hilden, Germany) RNeasy and Quanta biosciences' (Beverly, USA) qScript kit, respectively, according to the manufacturers' instructions. qPCR was performed on an Eppendorf (Hamburg, Germany) iCycler in 96-well format. Per reaction, 300 ng cDNA were diluted in a total volume of 19 µl qPCR master mix (ddH_2O with 200 µM of each dATP, dGTP, dCTP and dTTP, 100 nM fluorescin calibration dye, 7.5x SyBr Green, 4% DMSO, 1x PCR Rxn buffer, 3 mM $MgCl_2$, and 0.6 U Taq polymerase (Thermo Fisher Scientific)) and supplemented with 1 µl primer mix consisting of 5 µM forward and reverse primers (all IDT, Coralville, USA). Primer sequences were as follows: *18s* F: 5'-TTCCTTGGACCGGCGCAAG-3', R: 5'-GCCGCATCGCCGGTCGG-3'; *ITGA6* F: 5'-AAAGCCTGCTCAATCCCTGA-3', R: 5'-GTAAGTCAGCCACGCCAAAA-3'; *ITGAE* F: 5'-GGTTCTTTCTCCTTGGCACG-3', R: 5'-CATCTGCCCCAAAACCTTCC-3'; *ITGB1* F: 5'-AGCTTTAAAACCTGTGTGCCAT-3', R: 5'-CAAAAGGTCCCCATTCAGCAA-3'; *ITGB5* F: 5'-GGCTTGATCACAGCTCCCTA-3', R: 5'-GGACAACAAGCTGGATGTGG-3'; *ITGB8* F: 5'-AAGAGCAGTCACCTACCGAC-3', R: 5'-CGTTCGAGTGTACAACCAGC-3'; *GFAP* F: 5'-ATCGAGAAGGTTCGCTTCCT-3', R: 5'-CAGCCTCAGGTTGGTTTCAT-3'; *MAP2* F: 5'-AAAGAAAAGGCCCAAGCTAAA-3', R: 5'-GCTTCCAGACGAGGAGACA-3'; *NEUN* F: 5'-GGATGGATTTTATGGTGCTGA-3', R: 5'-ACATGGTTCCAATGCTGTAGG-3'; *NGN2* F: 5'-CTGGGTCTGGTACACGATTG-3', R: 5'-GGTTGTTGGCCTTCAGTCTA-3'; *PAX6* F: 5'-AATAACCTGCCTATGCAACCC-3', R: 5'-AACTTGAACTGGAACTGACACAC-3'; *SLC25A1* F: 5'-CCCCATGGAGACCATCAA-3', R: 5'-CCTGGTACGTCCCCTTCAG-3'; *SOX2* F: 5'-GTATCAGGAGTTGTCAAGGCAGAG-3', R: 5'-TCCTAGTCTTAAAGAGGCAGCAAAC-3'; *TUBB3* F: 5'-CCATCTTGCTGCCGACAC-3', R: 5'-CAATAAGACAGAGACAGGAG-3'; *VIM* F: 5'-TCTCTGAGGCTGCCAACCG-3', R: 5'-CGAAGGTGACGAGCCATTTCC-3'. qPCR reactions were run in triplicates and cycling conditions were as follows: 3 minutes at 95°C; 40 cycles of 15 seconds at 95°C, 20 seconds at 60°C and 30 seconds at 72°C; 1 minute at 95°C and 15 seconds at 55°C, followed by a temperature gradient to 95°C over the course of 20 minutes and finally 15 seconds at 95°C, before cooling down to 4°C. Ct values of the genes of interest were normalized to the house-keeping gene *18s* and transformed to mean fold changes using the Eq. $2^{-\Delta\Delta Ct}$. qPCR products were size-validated by gel electrophoresis.

Statistical Analysis

All statistical analyses were performed with R (version 3.5.1; the R foundation for statistical computing 2018). First, to determine whether variables met the assumptions of linear models, Kolmogorov-Smirnov's, Shapiro Wilk's and Levene's test, and/or F-test for normal distribution and homogeneity of variance were performed. Since data were not normally distributed, two-sided Wilcoxon rank sum tests

were calculated to compare two groups. Correlation was assessed using Kendall's τ. The significance level was set to $p < 0.05$. Multiple testing on the same set of data was not performed.

Statement of Ethical Approvals

The collection of human somatic material (*i.e.*, blood or fibroblasts) from healthy donors for iPSC reprogramming and iNSC conversion was in accordance with German law and approved by the ethics committee of the University of Bonn Medical Center (approval number: 275/08). All subjects gave written informed consent.

Declarations

Data Availability Statement

The AAV screening data will be deposited in the freely accessible online database SPIRIT (http://spirit.cladiac.com/aav.html) upon publication.

Author contributions

LJF, KB, DG and OB conceived and designed the study. LJF, VS, CAY, JS, MH and MM cultivated human cell programming-derived CNS cells for the study. LJF, KB and VSB performed experiments. LJF, KB, CS and SZ assembled and analyzed data. LJF, KB, DG and OB interpreted data and wrote the manuscript. All authors read and approved the final manuscript.

Acknowledgements

The authors thank Michaela Segschneider (LIFE & BRAIN GmbH) and Cornelia Thiele (Institute of Reconstructive Neurobiology, University of Bonn Medical Faculty & University Hospital Bonn) for providing cryo-preservedltNES and pre-differentiated ltNES-derived neuroglial differentiation cultures. Furthermore, we thank Nils Braun (Institute of Reconstructive Neurobiology, University of Bonn Medical Faculty & University Hospital Bonn) for providing the NR6AI-C-term-3xFLAG plasmid as cloning template. We further thank Natalia Garcia Perez (Institute of Reconstructive Neurobiology, University of Bonn Medical Faculty & University Hospital Bonn) and Lydia Fischer (Institute of Experimental Epileptology and Cognition Research, University of Bonn Medical Faculty & University Hospital Bonn) for supporting AAV titration.

DG is grateful for support from the German Research Foundation (DFG; Collaborative Research Centers SFB1129 [TP2/16, Projektnummer 240245660] and TRR179 [TP18, Projektnummer 272983813], Cluster of Excellence CellNetworks [EXC81]). KB and DG kindly acknowledge additional funding by the German Center for Infection Research (DZIF, BMBF, TTU-HIV 04.815).OB appreciates support from the European Union's Horizon 2020 research and innovation program under grant agreement no 874758 (NSC-Reconstruct) and the National Institutes of Health, USA (award no. R01 NS100514).

Competing interests

DG is a co-founder, shareholderand chief scientific officer of AaviGen GmbH. OB is co-founder,shareholder and CEO of LIFE & BRAIN GmbH. KB and DG are inventors on pending patent applications related to the AAV variants used in this work, as are MM and OB for the differentiation paradigm used to produce iPSdMiG. CS is co-founder, shareholder and chief execution officer of CLADIAC GmbH and SSE. SZ is co-founder and shareholder of CLADIAC GmbH and KINSYS GmbH. All other authors declare no competing interests.

References

1. Takahashi, K. & Yamanaka, S. Induction of pluripotent stem cells from mouse embryonic and adult fibroblast cultures by defined factors. *Cell***126**, 663–676 (2006).
2. Takahashi, K. *et al.* Induction of pluripotent stem cells from adult human fibroblasts by defined factors. *Cell***131**, 861–872 (2007).
3. Flitsch, L. J., Laupman, K. E. & Brüstle, O. Transcription factor-based fate specification and forward programming for neural regeneration. *Front. Cell. Neurosci.***14**, 1–22 (2020).
4. Flitsch, L. J. & Brüstle, O. Evolving principles underlying neural lineage conversion and their relevance for biomedical translation. *F1000Research***8**, 1548 (2019).
5. Mertens, J., Marchetto, M. C., Bardy, C. & Gage, F. H. Evaluating cell reprogramming, differentiation and conversion technologies in neuroscience. *Nat. Rev. Neurosci.***17**, 424–437 (2016).
6. Barker, R. A., Götz, M. & Parmar, M. New approaches for brain repair - from rescue to reprogramming. *Nature***557**, 329–334 (2018).
7. Mattugini, N. *et al.* Inducing different neuronal subtypes from astrocytes in the injured mouse cerebral cortex. *Neuron***103**, 1086-1095.e5 (2019).
8. Rivetti Di Val Cervo, P. *et al.* Induction of functional dopamine neurons from human astrocytes in vitro and mouse astrocytes in a Parkinson's disease model. *Nat. Biotechnol.***35**, 444–452 (2017).
9. Rezvani, M. *et al.* In vivo hepatic reprogramming of myofibroblasts with AAV vectors as a therapeutic strategy for liver fibrosis. *Cell Stem Cell***18**, 809–816 (2016).
10. Senís, E. *et al.* AAV vector-mediated in vivo reprogramming into pluripotency. *Nat. Commun.***9**, 1–14 (2018).
11. Kotterman, M. A. & Schaffer, D. V. Engineering adeno-associated viruses for clinical gene therapy. *Nat. Rev. Genet.***15**, 445–451 (2014).
12. Wang, D., Tai, P. W. L. & Gao, G. Adeno-associated virus vector as a platform for gene therapy delivery. *Nat. Rev. Drug Discov.***18**, 358–378 (2019).
13. Hammond, S. L., Leek, A. N., Richman, E. H. & Tjalkens, R. B. Cellular selectivity of AAV serotypes for gene delivery in neurons and astrocytes by neonatal intracerebroventricular injection. *PLoS One***12**, 1–22 (2017).

14. Kunze, C. *et al.* Synthetic AAV/CRISPR vectors for blocking HIV-1 expression in persistently infected astrocytes. *Glia***66**, 413–427 (2018).
15. Duong, T. T. *et al.* Comparative AAV-EGFP transgene expression using vector serotypes 1–9, 7M8, and 8b in human pluripotent stem cells, RPEs, and human and rat cortical neurons. *Stem Cells Int.***2019**, (2019).
16. Rapti, K. *et al.* Effectiveness of gene delivery systems for pluripotent and differentiated cells. *Mol. Ther. - Methods Clin. Dev.***2**, 14067 (2015).
17. Hudry, E. & Vandenberghe, L. H. Therapeutic AAV gene transfer to the nervous system: A clinical reality. *Neuron***101**, 839–862 (2019).
18. Li, C. & Samulski, R. J. Engineering adeno-associated virus vectors for gene therapy. *Nat. Rev. Genet.***21**, 255–272 (2020).
19. Börner, K. *et al.* Pre-arrayed pan-AAV peptide display libraries for rapid single-round screening. *Mol. Ther.***28**, 1016–1032 (2020).
20. Sheng, C. *et al.* A stably self-renewing adult blood-derived induced neural stem cell exhibiting patternability and epigenetic rejuvenation. *Nat. Commun.***9**, 4047 (2018).
21. Reinhardt, P. *et al.* Derivation and expansion using only small molecules of human neural progenitors for neurodegenerative disease modeling. *PLoS One***8**, e59252 (2013).
22. Koch, P., Opitz, T., Steinbeck, J. A., Ladewig, J. & Brustle, O. A rosette-type, self-renewing human ES cell-derived neural stem cell with potential for in vitro instruction and synaptic integration. *Proc. Natl. Acad. Sci.***106**, 3225–3230 (2009).
23. Gorris, R. *et al.* Pluripotent stem cell-derived radial glia-like cells as stable intermediate for efficient generation of human oligodendrocytes. *Glia***63**, 2152–2167 (2015).
24. Peitz, M., Krutenko, T. & Brüstle, O. Protocol for the standardized generation of forward programmed cryopreservable excitatory and inhibitory forebrain neurons. *STAR Protoc.***1**, 100038 (2020).
25. Cearley, C. N. *et al.* Expanded repertoire of AAV vector serotypes mediate unique patterns of transduction in mouse brain. *Mol. Ther.***16**, 1710–1718 (2008).
26. Shi, W. & Bartlett, J. S. RGD inclusion in VP3 provides adeno-associated virus type 2 (AAV2)-based vectors with a heparan sulfate-independent cell entry mechanism. *Mol. Ther.***7**, 515–525 (2003).
27. Stachler, M. D. & Bartlett, J. S. Mosaic vectors comprised of modified AAV1 capsid proteins for efficient vector purification and targeting to vascular endothelial cells. *Gene Ther.***13**, 926–931 (2006).
28. Sayroo, R. *et al.* Development of novel AAV serotype 6 based vectors with selective tropism for human cancer cells. *Gene Ther.***23**, 18–25 (2016).
29. Kunji, E. R. S., King, M. S., Ruprecht, J. J. & Thangaratnarajah, C. The SLC25 carrier family: Important transport proteins in mitochondrial physiology and pathology. *Physiology***35**, 302–327 (2020).
30. Palmieri, F. Mitochondrial transporters of the SLC25 family and associated diseases: A review. *J. Inherit. Metab. Dis.***37**, 565–575 (2014).

31. Zhang, Y. *et al.* Rapid single-step induction of functional neurons from human pluripotent stem cells. *Neuron***78**, 785–798 (2013).
32. Grande, A. *et al.* Environmental impact on direct neuronal reprogramming in vivo in the adult brain. *Nat. Commun.***4**, 2373 (2013).
33. Götz, M., Stoykova, A. & Gruss, P. Pax6 controls radial glia differentiation in the cerebral cortex. *Neuron***21**, 1031–1044 (1998).
34. Heins, N. *et al.* Glial cells generate neurons: The role of the transcription factor Pax6. *Nat. Neurosci.***5**, 308–315 (2002).
35. Hack, M. A., Sugimori, M., Lundberg, C., Nakafuku, M. & Götz, M. Regionalization and fate specification in neurospheres: The role of Olig2 and Pax6. *Mol. Cell. Neurosci.***25**, 664–678 (2004).
36. Kallur, T., Gisler, R., Lindvall, O. & Kokaia, Z. Pax6 promotes neurogenesis in human neural stem cells. *Mol. Cell. Neurosci.***38**, 616–628 (2008).
37. Osumi, N., Shinohara, H., Numayama-Tsuruta, K. & Maekawa, M. Concise review: Pax6 transcription factor contributes to both embryonic and adult neurogenesis as a multifunctional regulator. *Stem Cells***26**, 1663–1672 (2008).
38. Sansom, S. N. *et al.* The level of the transcription factor Pax6 is essential for controlling the balance between neural stem cell self-renewal and neurogenesis. *PLoS Genet.***5**, 20–23 (2009).
39. Kronenberg, G. *et al.* Modulation of fate determinants Olig2 and Pax6 in resident glia evokes spiking neuroblasts in a model of mild brain ischemia. *Stroke***41**, 2944–2949 (2010).
40. Thakurela, S. *et al.* Mapping gene regulatory circuitry of Pax6 during neurogenesis. *Cell Discov.***2**, 15045 (2016).
41. Excoffon, K. J. D. A. *et al.* Directed evolution of adeno-associated virus to an infectious respiratory virus. *Proc. Natl. Acad. Sci. U. S. A.***106**, 3865–3870 (2009).
42. Asuri, P. *et al.* Directed evolution of adeno-associated virus for enhanced gene delivery and gene targeting in human pluripotent stem cells. *Mol. Ther.***20**, 329–338 (2012).
43. Jang, J. H. *et al.* An evolved adeno-associated viral variant enhances gene delivery and gene targeting in neural stem cells. *Mol. Ther.***19**, 667–675 (2011).
44. Ravindra Kumar, S. *et al.* Multiplexed Cre-dependent selection yields systemic AAVs for targeting distinct brain cell types. *Nat. Methods***17**, 541–550 (2020).
45. Latour, Y. L. *et al.* Human GLB1 knockout cerebral organoids: A model system for testing AAV9-mediated GLB1 gene therapy for reducing GM1 ganglioside storage in GM1 gangliosidosis. *Mol. Genet. Metab. Reports***21**, (2019).
46. Chen, Y. C. *et al.* A NeuroD1 AAV-based gene therapy for functional brain repair after ischemic injury through in vivo astrocyte-to-neuron conversion. *Mol. Ther.***28**, 1–18 (2019).
47. Wu, Z. *et al.* Gene therapy conversion of striatal astrocytes into GABAergic neurons in mouse models of Huntington's disease. *Nat. Commun.***11**, 1–18 (2020).

48. Weinmann, J. *et al.* Identification of a myotropic AAV by massively parallel in vivo evaluation of barcoded capsid variants. *Nat. Commun.***11**, 5432 (2020).
49. Kremer, L. P. *et al.* In vivo high-throughput screening of novel adeno-associated viral capsids identifies variants for transduction of adult neural stem cells within the subventricular zone. *Mol. Ther. - Methods Clin. Dev.* (2021). doi:10.1016/j.omtm.2021.07.001
50. Powell, S. K., Samulski, R. J. & McCown, T. J. AAV capsid-promoter interactions determine CNS cell-selective gene expression in vivo. *Mol. Ther.***28**, 1373–1380 (2020).
51. Grimm, D. Production methods for gene transfer vectors based on adeno-associated virus serotypes. *Methods***28**, 146–157 (2002).
52. Amoasii, L. *et al.* Single-cut genome editing restores dystrophin expression in a new mouse model of muscular dystrophy. *Sci. Transl. Med.***9**, eaan8081 (2017).
53. Börner, K. *et al.* From experimental setup to bioinformatics: An RNAi screening platform to identify host factors involved in HIV-1 replication. *Biotechnol. J.***5**, 39–49 (2010).

Figures

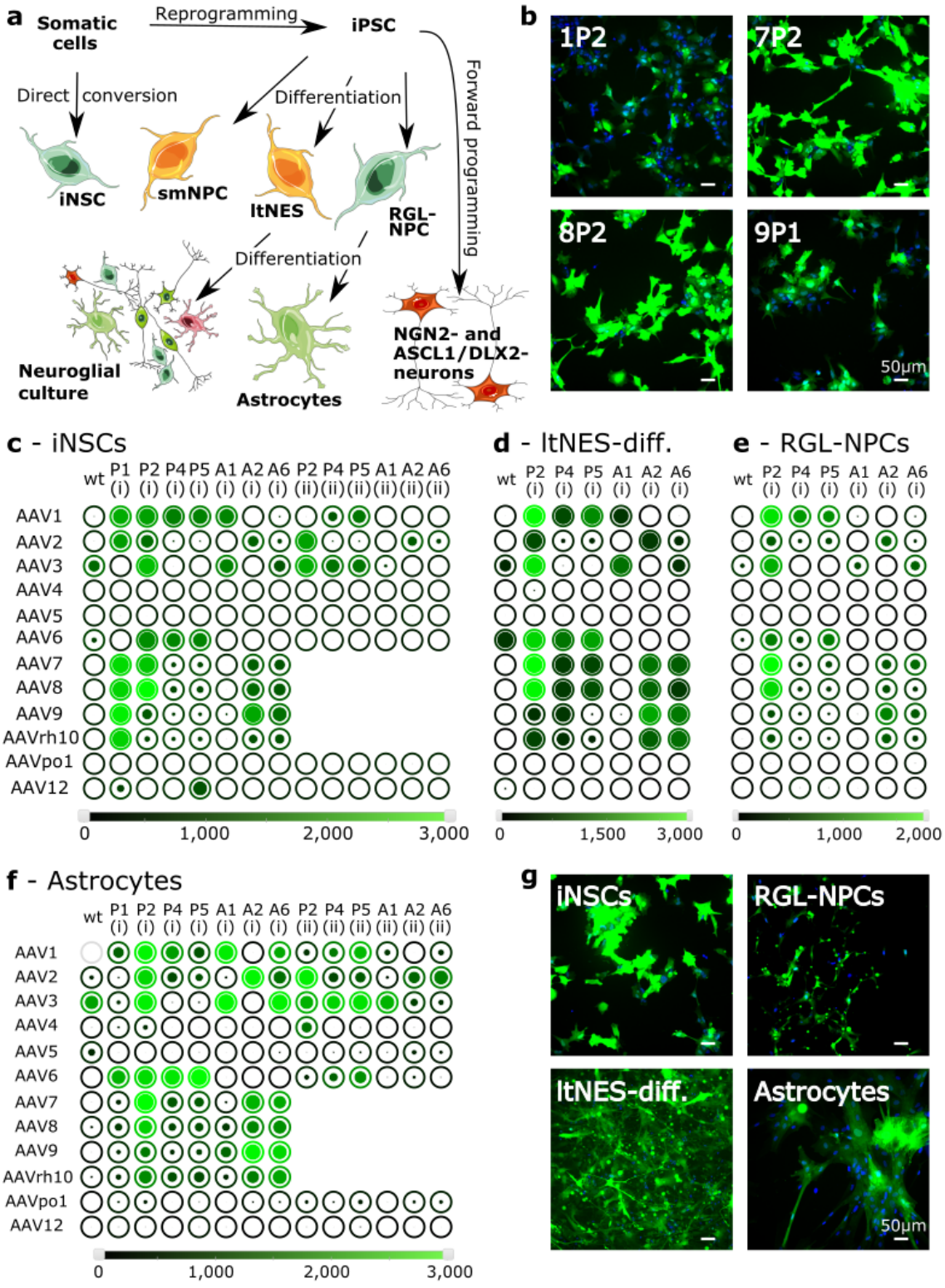

Figure 1

Use of pre-arrayed AAV screening panels to identify lead candidates for efficient transduction of human cell programming-derived neural cell types. (a) Schematic representation of the variety of cell programming-derived human cell types tested in this study, as well as their amenability to AAV transduction with the variants used in this screen (green,orange and red colors indicate good, intermediateand poor transducibility, respectively). Components of the figure were adapted from Servier

Medical Art (https://smart.servier.com).(b) Representative immunofluorescence images of iNSCs after transduction with the AAV variants AAV1P2, 7P2, 8P2 and 9P1. Fluorescence micrographs are depicted at the same gain to visualize differences.(c-f) Bubble charts representing transduction efficiencies (circle filling; in %) and absolute expression levels (color scalebar; mean gray value of all cells in the analyzed images)of all screened AAV-YFP variants in directly converted iNSCs (c), ltNES-derived differentiation cultures (ltNES-diff.) consisting of both, neuronal and glial cells (d),iPSC-derived RGL-NPCs (e) andRGL-NPC-derived astrocytes (f).wt = wild-type.Inserted peptides (P1, P2, P4, P5, A1, A2, A6) and insertion sites (i, ii) are described in Supplementary Tables S1 and S2, respectively.(g) Representative immunofluorescence images of iNSCs, RGL-NPCs, differentiated ltNESculturescomprising neurons as well as astrocytes, and pure iPSC-derived astrocytic cultures after transduction with the lead AAV variant 7P2.

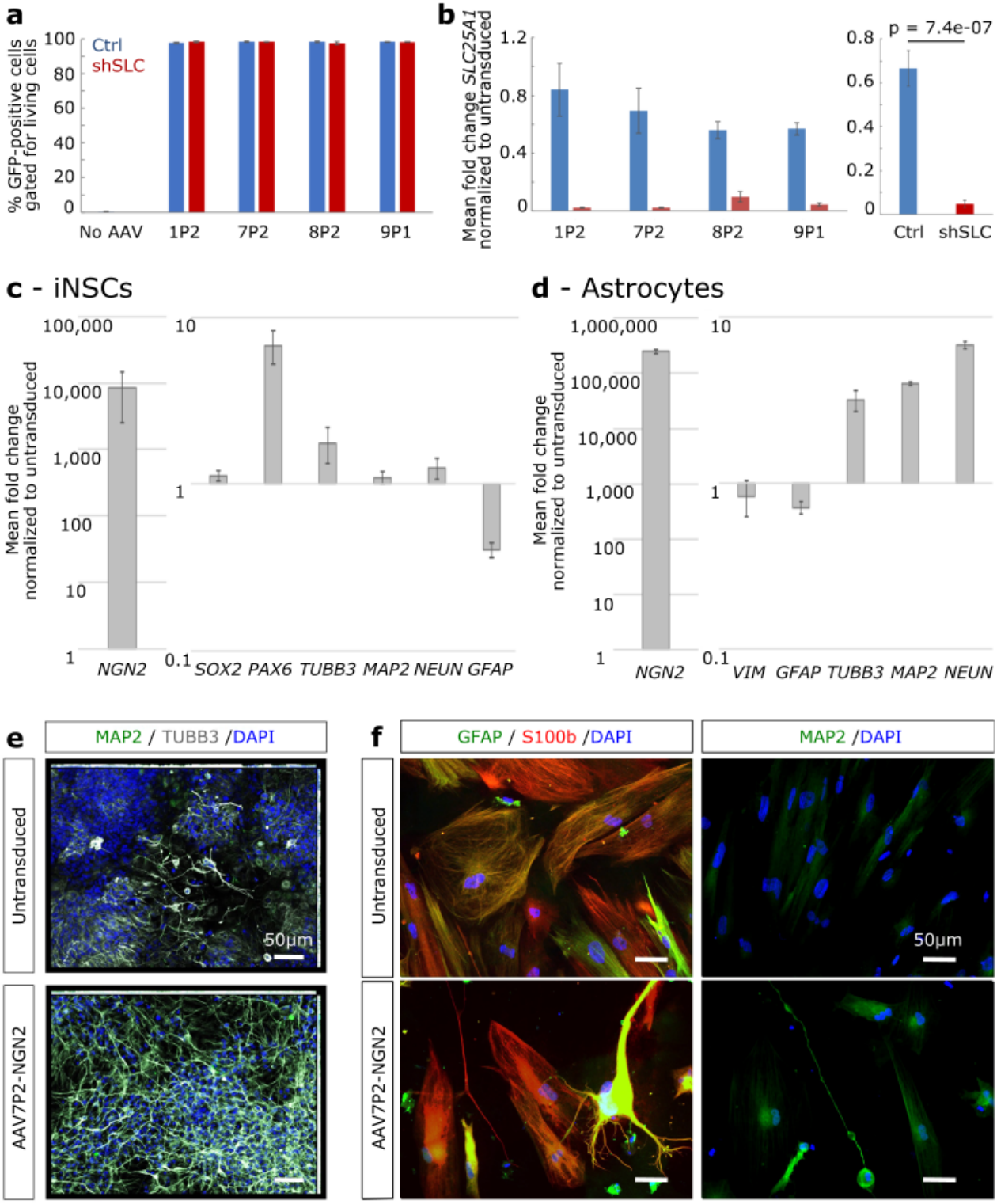

Figure 2

AAVs selected from the screen are capable of achieving shRNA-mediated gene knockdown and transgene overexpression in iNSCs and astrocytes. (a)Transduction efficiencies in iNSCs with crude lysates of the lead candidate AAV variants AAV1P2, 7P2, 8P2 and 9P1 expressing GFP along with shRNA-SLC25A1 (shSLC) or a non-silencing control shRNA (Ctrl). Bar graph represents means ± standard error from N = 3 independent experiments per condition.(b)Expression of SLC25A1as measured by qPCR.Bar graph

represents means ± standard error from N = 3 independent experiments per condition.The graph's left panel depicts the individual data of all AAV variants tested here, whilst the panel on the right depicts the means of all Ctrl and shSLC vectors. Wilcoxonrank sum test was performed on the pooled dataset.(c, d) qPCR-based expression profiling of neuronal and glial markers afterfourteen days of AAV7P2-mediated NGN2 overexpression in spontaneously differentiating iNSCs (c) and iPSC-derived astrocyte cultures (d). Bar graphs represent means ± standard error of N = 4 from 2 independent experiments.(e, f)Exemplary imagesof immunofluorescence stainings against neuronal and/or glial markers in differentiating iNSCs (e) and iPSC-derived astrocyte cultures (f).

Supplementary Files

This is a list of supplementary files associated with this preprint. Click to download.

- AAVSupplement20210831submitted.pdf